Kriging 法を用いた高揚力装置の最適設計

鄭　信圭[1]、金崎　雅博[2]、村山　光宏[2]

[1] 東北大学流体科学研究所
[2] 宇宙航空研究開発機構総合技術研究本部

High Lift Device Optimization Design with Kriging Model

by
Shinkyu Jeong, Masahiro Kanazaki and Mitsuhiro Murayama

ABSTRACT

In this study, Kriging model is applied to an aerodynamic design of a high lift device. The position of a slat and a flap is optimized. The Kriging model is updated by selection of the maximum EI point. Sample points for the Kriging model are evaluated by using UPACS (Unified Platform for Aerospace Computational Simulation) multi-block solver developed in JAXA. The effect of each position parameter to the aerodynamic performance can be identified by 3D-plot of the Kriging model.

１. Introduction

Recently, optimization method using approximation models[1] attracts a large attention in the field of aircraft design. A designer can save a lot of computational time for objective function evaluation by using the approximation model, instead of the high-fidelity CFD solvers. However, it is apt to miss the true optimum in the design space if the exploration relies only on the estimated function values of the approximation model because these values include uncertainty at unknown points. For the robust exploration of the true optimum with the approximation model, both the estimated function value and its error should be considered at the same time.

The Kriging model[2-3], developed in the field of spatial statistic and geostatistics, has gained the popularity today. The Kriging model predicts the distribution of function values at an unknown point instead of the function values it self. From the distribution of function values, the function value and its uncertainty at unknown points can be estimated. By using these values, the balanced local and global search is possible. This concept is expressed using the criterion 'expected improvement (EI)'[4-5]. EI indicates the probability of a point being the true optimum in the design space. By selecting maximum EI point as an additional sample point of the Kriging model, the improvement of accuracy and the robust exploration of the true optimum can be achieved at the same time.

In this study, the Kriging model is applied to the optimization of the slat and the flap position in the multi-element airfoil. MDA30P30N airfoil is used as the baseline airfoil. Sample positions for the construction of the Kriging model are evaluated by using UPACS (Unified Platform for Aerospace Computational Simulation)[6] multi-block solver developed in JAXA. The effect of each position parameter to the aerodynamic performance can be identified by 3D-plot of the Kriging model.

2. Kriging Model

The present Kriging model expresses the unknown function y(x) as

$$y(\mathbf{x}) = \mu + Z(\mathbf{x}) \tag{1}$$

where $\mathbf{x}$ is an m-dimensional vector (m design variables), μ is a constant global model and $Z(\mathbf{x})$ represents a local deviation from the global model. In the model, the local deviation at an unknown point ($\mathbf{x}$) is expressed using stochastic processes. The sample points are interpolated with the Gaussian random function as the correlation function to estimate the trend of the stochastic processes. The correlation between $Z(\mathbf{x}^i)$ and $Z(\mathbf{x}^j)$ is strongly related to the distance between the two corresponding points, $\mathbf{x}^i$ and $\mathbf{x}^j$. However, the Euclidean distance is not used, because it weighs all design variables equally. In the Kriging model, a special weighted distance is used instead. The distance function between the point at $\mathbf{x}^i$ and $\mathbf{x}^j$ is expressed as

$$d(\mathbf{x}^i, \mathbf{x}^j) = \sum_{k=1}^{m} \theta_k \left| x_k^i - x_k^j \right|^2 \tag{2}$$

where θ_k $(0 \le \theta_k \le \infty)$ is the k_{th} element of the correlation vector parameter $\boldsymbol{\theta}$. By using the specially weighted distance and the Gaussian random function, the correlation between the point $\mathbf{x}^i$ and $\mathbf{x}^j$ is defined as

$$Corr\left[Z(\mathbf{x}^i), Z(\mathbf{x}^j)\right] = \exp\left[-d(\mathbf{x}^i, \mathbf{x}^j)\right] \tag{3}$$

The Kriging predictor is

$$\hat{y}(\mathbf{x}) = \hat{\mu} + \mathbf{r}'\mathbf{R}^{-1}(\mathbf{y} - \mathbf{1}\hat{\mu}) \tag{4}$$

where $\hat{\mu}$ is the estimated value of μ, $\mathbf{R}$ denotes the $n \times n$ matrix whose (i, j) entry is $Corr\left[Z(\mathbf{x}^i), Z(\mathbf{x}^j)\right]$. $\mathbf{r}$ is vector whose i_{th} element is

$$r_i(\mathbf{x}) \equiv Corr\left[Z(\mathbf{x}), Z(\mathbf{x}^i)\right] \tag{5}$$

and $\mathbf{y} = [y(x^1), \ldots\ldots, y(x^n)]$.
The detailed derivation of Eq. (4) can be found in [7].

The unknown parameter to be estimated for constructing the Kriging model is $\boldsymbol{\theta}$. This parameter can be estimated by maximizing the following likelihood function

$$Ln(\hat{\mu},\hat{\sigma}^2,\boldsymbol{\theta}) = -\frac{n}{2}\ln(2\pi) - \frac{n}{2}\ln(\hat{\sigma}^2) - \frac{1}{2}\ln(|\mathbf{R}|) - \frac{1}{2\hat{\sigma}^2}(\mathbf{y}-\mathbf{1}\hat{\mu})'\mathbf{R}^{-1}(\mathbf{y}-\mathbf{1}\hat{\mu}) \tag{6}$$

where $\mathbf{1}$ denotes an m-dimensional unit vector.

Maximizing the likelihood function is an m-dimensional unconstrained non-linear optimization problem. In this paper, the alternative method[8] is adopted to solve this problem.

For a given $\boldsymbol{\theta}$, $\hat{\mu}$ and $\hat{\sigma}^2$ can be defined as

$$\hat{\mu} = \frac{\mathbf{1}'\mathbf{R}^{-1}\mathbf{y}}{\mathbf{1}'\mathbf{R}^{-1}\mathbf{1}} \tag{7}$$

$$\hat{\sigma}^2 = \frac{(\mathbf{y}-\mathbf{1}\mu)'\mathbf{R}^{-1}(\mathbf{y}-\mathbf{1}\mu)}{n} \tag{8}$$

Next, vector $\boldsymbol{\theta}$ is updated by using

$$\boldsymbol{\theta}^{new} = \boldsymbol{\theta}^{old} + \mathbf{B}^{-1}\frac{\partial Ln}{\partial \boldsymbol{\theta}} \tag{9}$$

where

$$\frac{\partial Ln}{\partial \theta_k} = -\frac{1}{2}tr\left\{\frac{1}{\mathbf{R}}\frac{\partial \mathbf{R}}{\partial \theta_k}\right\} - \frac{1}{2\sigma^2}(\mathbf{y}-\mathbf{1}\mu)'\frac{1}{\mathbf{R}}\frac{\partial \mathbf{R}}{\partial \theta_k}\frac{1}{\mathbf{R}}(\mathbf{y}-\mathbf{1}\mu) \tag{10}$$

and the $(i,j)_{th}$ element of matrix $\mathbf{B}$ is $\frac{1}{2}t_{ij}$ with

$$t_{ij} = tr(\mathbf{R}^{-1}\frac{\partial \mathbf{R}}{\partial \theta_i}\mathbf{R}^{-1}\frac{\partial \mathbf{R}}{\partial \theta_j}). \tag{11}$$

For this updated $\boldsymbol{\theta}^{new}$, new values of $\hat{\mu}$ and $\hat{\sigma}^2$ can be calculated using Eq. (7) and (8). This routine is iterated until function Ln converges to a maximum value

The accuracy of the prediction value largely depends on the distance from sample points. Intuitively speaking, the closer point $\mathbf{x}$ to sample points, the more accurate is the prediction $\hat{y}(\mathbf{x})$. This intuition is expressed in following Equation.

$$s^2(\mathbf{x}) = \hat{\sigma}^2\left[1 - \mathbf{r}'\mathbf{R}^{-1}\mathbf{r} + \frac{(1-\mathbf{1}\mathbf{R}^{-1}\mathbf{r})^2}{\mathbf{1}'\mathbf{R}^{-1}\mathbf{1}}\right] \tag{12}$$

$s^2(\mathrm{x})$ is the mean squared error of the predictor. $s(\mathrm{x})$ indicates the uncertainty at the estimation point. The root mean squared error (RSME) is expressed as $s = \sqrt{s^2(\mathbf{x})}$.

3. Expected Improvement and Treatment of Constraint

In order to find the true optimum, the Kriging model uses both the estimated function value and the uncertainty at the points. Based on these values, the point having the largest probability of being global optimum is found. This concept is expressed by the criterion 'expected improvement (EI)'. The EI is express as follows:

$$E(I) = s\int_{-\infty}^{f_{\min}^n}(f_{\min} - z)\phi(z)dz \tag{13}$$

where $f_{\min}^n = \frac{y_{\min} - \hat{y}}{s}$, $z = \frac{y-\hat{y}}{s}$ and

$$I(x) = \begin{cases} [y_{\min} - y(x)] & if\ y(x) < y_{\min} \\ 0 & otherwise \end{cases} \tag{14}$$

To impose the constraint effects into the conventional EI criterion, the probability of satisfying the constraints is calculated on the Kriging model for constraints. If there is the constraint $c_i(x) > a_i$, the probability of satisfying this constraint[9] is

$$P(c_i(x) \geq a_i) = \frac{1}{s_i\sqrt{2\pi}}\int_{a_i}^{\infty} e^{-\frac{1}{2}\left(\frac{c_i(x)-a_i}{s_i}\right)^2} dc_i(x) = 1 - \Phi(\frac{\hat{c}_i(x) - a_i}{s_i}) \tag{15}$$

And the constraint imposed EI criterion is as follows:

$$E_c(I) = E(I)\cdot P(c_i(x) > a_i) \tag{16}$$

4. Optimization Problem

The optimization problem is to find the position of the slat and the flap where maximizing L/D subject to $Cl > Cl_{baseline}(= 4.1)$ at a specified condition (Mach=0.2 and AOA=16.21).

4.1. Definition of Design Variables

Total 6 design variables are used to define the position of the slat and the flap. Figure 1 show the baseline airfoil (MDA30P30A) and design variables. Search region of each design variable is defined as follows:

1) slat angle:
   $-10\text{deg.} \leq \Delta\theta_{slat} \leq 10\text{deg.}$
2) x displacement of slat:
   $-0.03 \leq \Delta x_{slat}/c \leq 0.02$
3) y displacement of slat:
   $-0.05 \leq \Delta y_{slat}/c \leq 0.05$
4) flap angle:
   $-10\text{deg.} \leq \Delta\theta_{flap} \leq 10\text{deg.}$
5) x displacement of flap:
   $-0.03 \leq \Delta x_{flap}/c \leq 0.05$
6) y displacement of flap:
   $-0.1 \leq \Delta y_{flap}/c \leq 0.01$

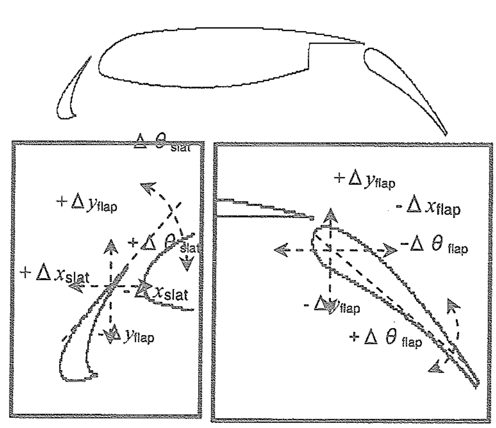

Figure 1. Baseline geometry and design variables

In this search region, total 20 sample points are selected by using the Latin hypercube sampling.

4.2 Evaluation

Evaluations of sample points for the Kriging model are performed by using UPACS (Unified Platform for the Aerospace Computation Simulation), a structured multi-block flow solver. UPACS was developed at Japan Aerospace Exploration Agency (JAXA; formerly National Aerospace Laboratory) as a common-base code for aerodynamic researcher.

In this study, Reynolds-averaged Navier-Stokes is used with the Spalart-Allmaras turbulent model. Flux is evaluated by Roe scheme with MUSCLE method for the third-order spatial accuracy.

The computation domain is typically decomposed into 33-36 sub-domains. Number of cells is about 10,000 in each domain. To reduce the mesh generation time, the dynamic mesh method is applied to deform the mesh around the baseline configuration, if mesh movement is not so large. If the mesh movement is large, the computational mesh is regenerated.

4.3 Optimization Procedure

The overall optimization procedure is shown in Fig. 2.

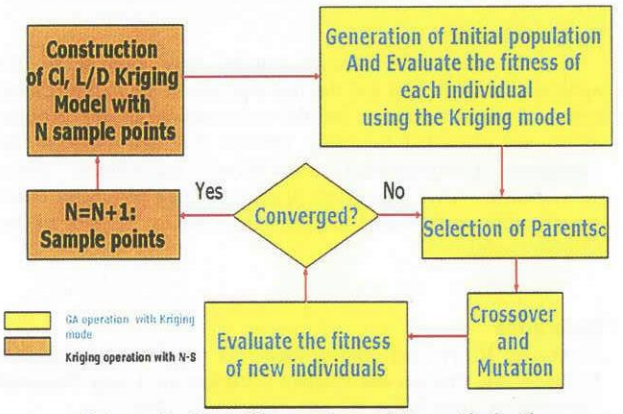

Figure 2. Overall procedure of the optimization

1. Kriging models are constructed for C_l and L/D with 24 sample points
2. GA operations[10]
   - Generation of initial population and evaluation of $E_c(I)$ and *Area ratio*
   - Selection of parents
   - Crossover and mutation
   - Evaluation of new individuals in Kriging models

When the generation exceeds 100, the point which gives maximum EI is selected as an additional sample point. This routine is iterated until the termination criterion is reached. In this study, termination criterion is the maximum number of additional sample points.

5. Results and Discussion

5.1 Initial Kriging model

Figure 3 show L/D plots against $\Delta\theta_{flap}$-$\Delta y_{flap}/c$, $\Delta\theta_{slat}$-$\Delta y_{slat}/c$ and $\Delta\theta_{slat}$-$\Delta\theta_{flap}$ predicted by the initial Kriging model with 20 sample points.

The maximum L/D point in Fig 3(a) is found around $\Delta\theta_{flap}$=-8. The local maximum is found around $\Delta\theta_{flap}$=3 and $\Delta y_{flap}/c$ = 0. According to the Fig 3(a), the angle of flap gives a large effect to the L/D performance of this airfoil. On the other hand, the y-displacement of flap gives little effect to the L/D performance of this airfoil. In case of Fig. 3(b), the maximum is found at $\Delta\theta_{slat}$=10. and $\Delta y_{slat}/c$=-0.04. However, the effect of the slat is smaller than the effect of the flap. Fig.3(c) shows that the change of the flap angle gives a larger effect than that of the slat angle.

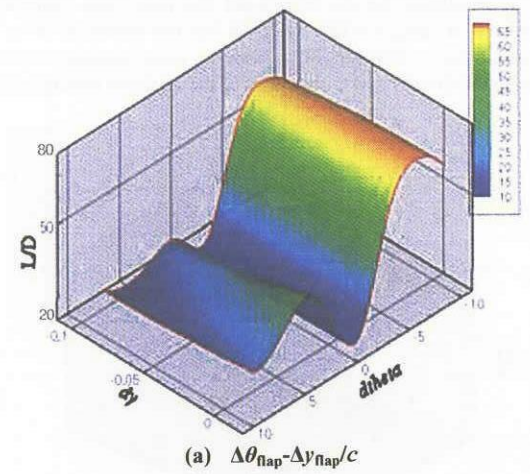

(a) $\Delta\theta_{flap}$-$\Delta y_{flap}/c$

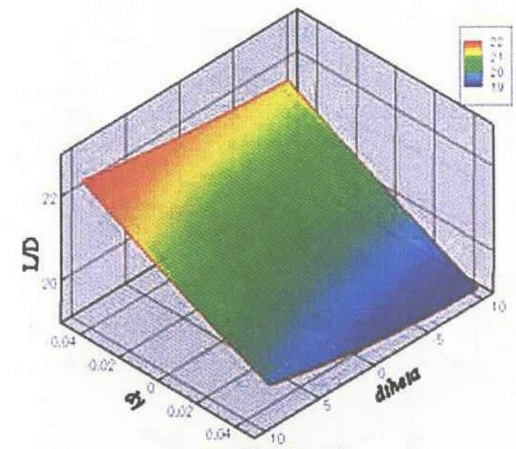

(b) $\Delta\theta_{slat}$-$\Delta y_{slat}/c$

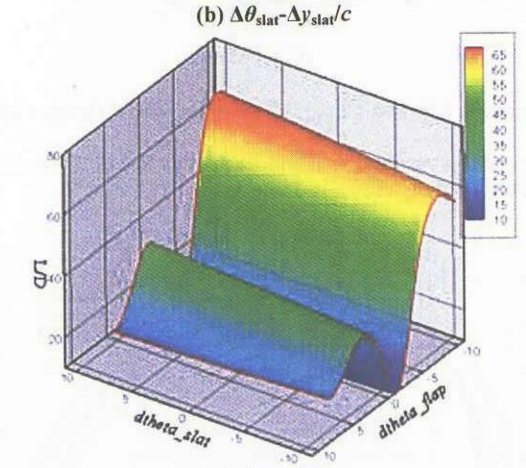

(c) $\Delta\theta_{slat}$-$\Delta\theta_{flap}$

Figure 3. L/D plots predicted by the initial Kriging model

5.2 Improved Kriging Model

Figure. 4 shows the L/D and the Cl plot in the improved Kriging model with 5 additional sample points. In Fig. 4(a), another local maximum around $\Delta\theta_{flap}$=0, Δy_{flap}=0 which was not found in Fig. 3(a) is shown. It means that the balanced local and global search has been done by adding the additional sample points. In the improved Kriging model, two positions which show high L/D performance are found. According to Fig. 4(b), Cl at $\Delta\theta_{flap}$=0, Δy_{flap}=0 is higher than Cl at $\Delta\theta_{flap}$=-0.02, Δy_{flap}=-8. This result suggests that the baseline configuration is useful for normal landing condition. On the other hand, this result also suggests that the design at $\Delta\theta_{flap}$=-0.02, Δy_{flap}=-8 has the potential to be used for go-around (retrial landing caused by some troubles) condition because the drag is lower than that of the baseline configuration.

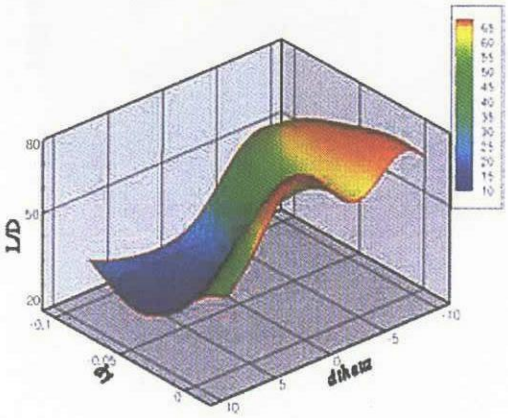

(a) L/D plot

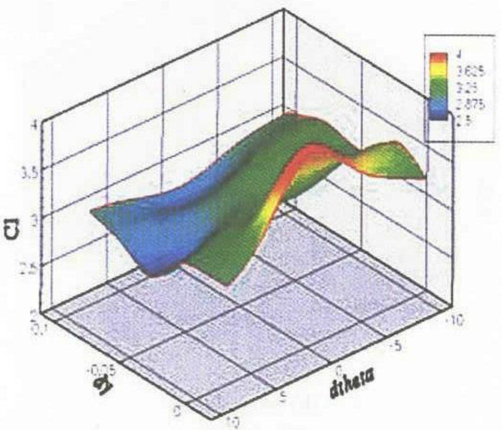

(b) Cl plot

Figure 4. L/D and Cl plot by the improved Kriging model

The positions are compared with each other in Fig. 5. The Cl and L/D performances shown in Table 1.

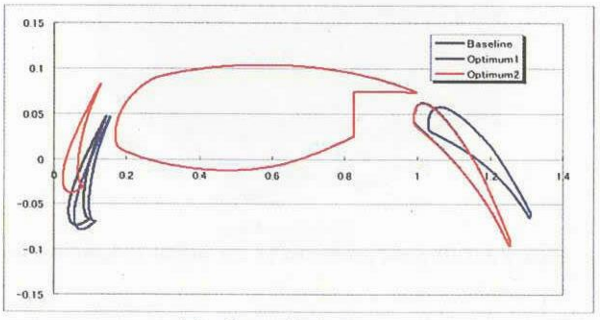

(a) Overall view

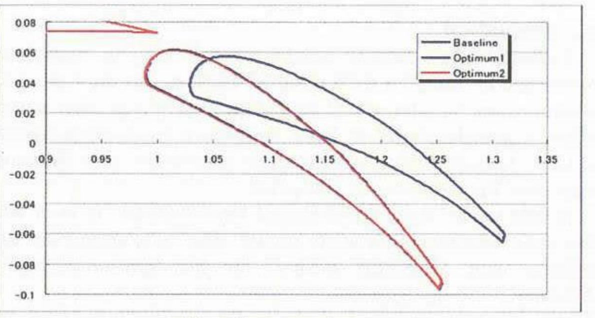

(b) Close up view

Figure 5. Position comparison

Table 1. Comparison of aerodynamic performances

	Baseline	Optimum1	Optimum2
Cl	4.103	3.559	4.113
L/D	78.088	78.427	78.091

6. Conclusion

In this study, the Kriging model was applied to the optimization of the slat and the flap position in the multi-element airfoil. Sample positions for the construction of the Kriging model are evaluated by using UPACS (Unified Platform for Aerospace Computational Simulation) multi-block solver developed in JAXA. The effect of each position parameter to the aerodynamic performance can be identified by 3D-plot of the Kriging model.

Reference

1) Myers, R. H. and Montgomery, D. C, *Response Surface Methodology*: Process and Product Optimization Using Designed Experiments, John Wiley & Sons, New York, 1995.

2) Timothy, W. S., Timothy M. M., John, J. K. and Farrokh, M, "Comparison of Response Surface And Kriging Models for Multidisciplinary Design Optimization," AIAA paper 98-4755.

3) Sack, J., Welch, W. J., Mitchell, T. J. and Wynn, H. P., "Design and analysis of computer experiments (with discussion)," Statistical Science 4, 1989, pp. 409-435.

4) Matthias, S., William, J. W. and Donald, R. J., "Global Versus Local Search in Constrained Optimization of Computer Models," *New Developments and Applications in Experimental Design*, edited by N. Flournoy, W.F. Rosenberger, and W.K. Wong , Institute of Mathematical Statistics, Hayward, California, Vol. 34, 1998, pp. 11-25.

5) Donald, R. J., Matthias S and William J. W, "Efficient Global Optimization of Expensive Black-Box Function," *Journal of global optimization*, Vol. 13, 1998, pp. 455-492.

6) Takaki, R., Yamatoto, K., Yamane, T., Enonoto, S. and Mukai, J., "Development of the UPACS CFD Environment," *Proceeding of ISHPC 2003*, Springer, 2003, pp. 307-319.

7) Koehler, J and Owen, A. Computer experiments, in S. Ghosh and C. R. Rao (eds.), *Handbook of Statistics*, 13: *Design and Analysis of Experiments*, Elsevier, Amsterdam, 1996, pp. 261-308.

8) Mardia, K. V. and R. J. Marshall, "Maximum likelihood estimation of models for residual covariance in Spatial regression," *Biometrika* Vol. 71, 1984, pp. 135-146.

9) Matthias, S., "Computer Experiments and Global Optimization," Ph.D Dissertation, Statistic and Actuarial Science Dept., University of Waterloo, Waterloo, Ontario, 1997.

10) Goldberg, D. E., "Genetic Algorithms in Search, Optimization & Machine Learning," Addison-Wesley Publishing, Inc., Reading, Jan., 1989.